

Journal of Materials Chemistry B

Accepted Manuscript



This is an *Accepted Manuscript*, which has been through the Royal Society of Chemistry peer review process and has been accepted for publication.

Accepted Manuscripts are published online shortly after acceptance, before technical editing, formatting and proof reading. Using this free service, authors can make their results available to the community, in citable form, before we publish the edited article. We will replace this *Accepted Manuscript* with the edited and formatted *Advance Article* as soon as it is available.

You can find more information about *Accepted Manuscripts* in the [Information for Authors](#).

Please note that technical editing may introduce minor changes to the text and/or graphics, which may alter content. The journal's standard [Terms & Conditions](#) and the [Ethical guidelines](#) still apply. In no event shall the Royal Society of Chemistry be held responsible for any errors or omissions in this *Accepted Manuscript* or any consequences arising from the use of any information it contains.

Ultra-Effective Photothermal Therapy for Prostate Cancer cells using Dual Aptamer-Modified Gold Nanostars

Cite this: DOI: 10.1039/x0xx00000x

Hunho Jo,[§] Hyungjun Youn,[§] Seonghwan Lee, and Changill Ban*

Received 00th January 2012,
Accepted 00th January 2012

DOI: 10.1039/x0xx00000x

www.rsc.org/

Currently, although various studies related to nanoparticles-based photothermal therapy have been actively performed, an epoch-making photothermolysis therapy exhibiting both high selectivity and efficiency has yet not been discovered. For the first time, we developed novel valuable therapeutic complexes, namely, dual aptamer-modified gold nanostars, for the targeting of prostate cancers, including PSMA(+) and PSMA(-) cells. The synthesized probes were characterized through several techniques, including UV-VIS spectral analysis, DLS analysis, zeta potential measurements, and TEM imaging, and were subsequently subjected to cytotoxicity tests, cell uptake confirmation, and *in vitro* photothermal therapy. The homogeneously well-fabricated nanostars presented high selectivity to prostate cancer cells and extremely high efficiency for therapy using an 808 nm laser under an irradiance of 0.3 W/cm², which is lower than the permitted value of skin (0.329 W/cm²). It is anticipated that this novel photothermal agent will become the general platform for targeted therapy.

Introduction

Noninvasive photothermal therapy (PTT) using near-infrared (NIR) light has received considerable attentions because it can efficiently kill target cells and reduce unwanted damage to surrounding cells, which is in contrast to other treatments, such as chemotherapy and radiation therapy.¹⁻⁷ Among various photothermal agents, gold nanostructures have been known as valuable materials due to their high production of heat by NIR radiation and the enhancement of the damage induced by radiation.⁸⁻¹⁰ In particular, star-shaped gold nanoparticles, denoted gold nanostars (AuNS), exhibit miscellaneous advantages, such as tunable plasmon bands, a tremendously high two-photon action cross section, and a large absorption-to-scattering ratio in response to NIR radiation.¹¹⁻¹⁵ This superiority makes AuNS one of the most powerful photothermolysis probes applicable to diverse *in vitro* and *in vivo* hyperthermia therapies.^{16, 17}

Prostate cancer has globally issued as one of the foremost causes of cancer-related death in men, especially in the UK and the United States; thus, the development of a highly effective and selective remedy for this disease have been strongly demanded.^{18, 19} Among several biomarkers for particularized therapy, prostate-specific membrane antigen (PSMA), a type II integral membrane glycoprotein associated with a higher tumor grade, has been broadly targeted in numerous treatments for prostate cancers, which has resulted in a notable increase in the number of associated studies.²⁰⁻²³ Since PSMA is only overexpressed in androgen-independent prostate cancers, the development of specific therapies for PSMA(-) cell lines has

seldom been carried out.^{24, 25} For complete cures for all types of prostate cancers, simultaneous targeting aimed at both PSMA(+) and PSMA(-) cancer cells is absolutely indispensable and has great importance in clinical demonstration.

To attain efficacious targeting, antibodies toward butt molecules have been widely employed in various therapies. However, because these antibodies have shown serious problems, such as instability due to changes in temperature, high developmental cost, and difficult chemical modifications, aptamers, oligonucleic acid or peptide molecules that can bind to specific target molecules, have been recently utilized as substitutes.²⁶⁻²⁸ An anti-PSMA RNA aptamer (A10) and a peptide aptamer (DUP-1) were previously identified as aptamers for PSMA(+) and PSMA(-), respectively.^{29, 30} Our group for the first time combined these two aptamers for the synchronous targeting of both PSMA(+) and PSMA(-) cancers and achieved remarkable results.^{31, 32}

For the design of a powerful photothermal probe that can selectively and effectively target both types of prostate cancer cells, we introduced dual aptamers into AuNS (Fig. 1). Until recently, almost all of the photothermal therapies used laser power greater than the well-known standard thresholds, which are based on the maximal permissible exposure (MPE) of skin established by the American National Standards Institutes.³³ In previous hyperthermia therapies, it was applied to the aimed cancers that fairly higher irradiations of 1.5-80 W/cm² than the MPE of skin (0.329 W/cm² at 808 nm).³⁴⁻³⁹ Even though the Vo-Dinh group has reported the impressive result that peptide-functionalized AuNS can represent photothermolysis under an

irradiance of 0.2 W/cm^2 , which is lower than the MPE of skin (0.4 W/cm^2 at 850 nm), the modified-AuNS did not exhibit selectivity to the specific targeted cancer.⁴⁰ Photothermal therapy with both high selectivity and efficiency simultaneously has not yet been developed for the specific target, particularly prostate cancer. Newly synthesized dual aptamers-modified AuNS (Dual-AuNS) showed excellent selectivity to only PSMA(+) and PSMA(-) prostate cancer cells and extreme efficiency in photothermolysis using a 808 nm NIR laser under an irradiation power of 0.3 W/cm^2 , markedly lower than the MPE of skin. In this work, we characterized ineptively devised aptamer-AuNS using various techniques and verified the efficacy of the probe via an MTT assay and microscopic analysis.

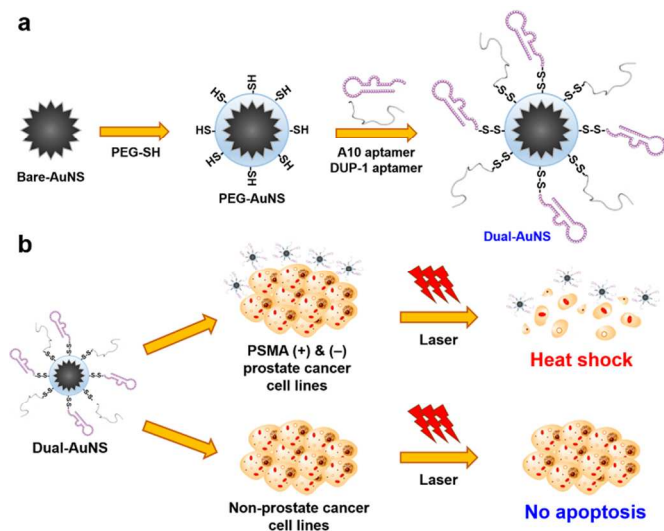


Fig. 1 (a) Functionalization of AuNS. Bare-AuNS were coated with PEG, and A10 and DUP-1 aptamers were then immobilized. (b) Selective photothermolysis for only PSMA(+) and PSMA(-) prostate cancer cells by Dual-AuNS.

Experimental section

Material

Gold(III) chloride, L-ascorbic acid, thiazolyl blue tetrazolium bromide, paraformaldehyde, glutaraldehyde, sodium cacodylate, and *O*-[2-(3-mercaptopropionylamino)ethyl]-*O'*-methylpolyethylene glycol (M_w 5000) were purchased from Sigma-Aldrich (USA). Silver nitrate was purchased from Kojima chemicals (Japan). Hydrochloric acid and ethyl alcohol were obtained from Wako (Japan). Trypan blue was bought from Invitrogen (USA). Nitric acid was procured from Samchun Chemical (Korea). RPMI-1640, penicillin G, streptomycin, and fetal bovine serum (FBS) were purchased from Hyclone (USA). Dimethyl sulfoxide was obtained from Kanto chemical (Japan).

Preparation of gold nanostars

Gold nanostars (AuNS) were prepared through a seed-mediated growth method.¹³ Prior to their synthesis, all of the glassware was washed with a 3:1 mixture of $\text{HCl}:\text{HNO}_3$ and rinsed with deionized water. For the synthesis of the seed solution, 1 mL of trisodium citrate (final 1.52 mM) was rapidly added to 100 mL of boiling 0.40 mM gold(III) chloride solution under vigorous stirring.⁴¹ After the color of the solution changed from pale

yellow to red, the solution was refluxed and cooled to room temperature (RT) under gentle stirring. The concentration of the seeds was measured via UV-VIS spectroscopy (Libra S22, Biochrom) at 520 nm . To prepare AuNS, $100 \mu\text{L}$ of the seed solution ($A_{520}=2.80$) was added to a mixture containing 10 mL of 0.25 mM HAuCl_4 and $10 \mu\text{L}$ of 1 M HCl under mild stirring. Then, $100 \mu\text{L}$ of 3 mM AgNO_3 and $50 \mu\text{L}$ of 100 mM ascorbic acid were simultaneously supplemented to the mixture, and the resulting mixture was allowed to incubate for 30 s at RT to yield a change in the color from light red to greenish-black. The centrifugation of the solution at $5,000 \text{ rpm}$ for 15 min stopped the nucleation of AuNS. Freshly synthesized AuNS were resuspended with deionized water and then filtered through a $0.22 \mu\text{m}$ nitrocellulose membrane. The concentration of AuNS was determined via a spectroscopic method.

Immobilization of dual aptamers on gold nanostars

For the PEGylation of AuNS, *O*-[2-(3-mercaptopropionylamino)ethyl]-*O'*-methylpolyethylene glycol (M_w 5000, final concentration of $5 \mu\text{M}$) was incubated with AuNS for 10 min under gentle shaking at RT. PEGylated AuNS (PEG-AuNS) were centrifugally washed and then resuspended in distilled water. To specifically target both types of prostate cancer cells, namely PSMA(+) and PSMA(-) cells, two aptamers were conjugated to PEG-AuNS via disulfide bonds. Thiol-modified A10 (5'-thiol-GGGAGGACGAUGCAGCAUGCAUGUUUACGUCACUCCUUGUCAUCCUCAUCGGC-3') was purchased from IDT (USA), and the cysteine-modified DUP-1 (CFRPNRAQDYNTN) aptamer was bought from Anygen (Korea). These aptamers were used without further purification. Then, $1 \mu\text{M}$ A10 aptamer and $2 \mu\text{M}$ DUP-1 were incubated with 1 nM PEG-AuNS in buffer containing 0.1% (v/v) Tween 20, 300 mM NaCl , and 10 mM phosphate buffer (pH 7.4) for 48 h at RT.⁴² The resulting nanoparticles (Dual-AuNS) were then centrifugally washed twice, resuspension in distilled water, and stored at $4 \text{ }^\circ\text{C}$.

Characterization of dual aptamer-modified gold nanostars

The TEM images of Dual-AuNS were taken using a JEM-1011 instrument (JEOL, Tokyo, Japan). The surface charges of Bare-AuNS, PEG-AuNS, and Dual-AuNS were verified in PBS buffer (pH 7.4) by zeta potential measurements using a Zetasizer Nano Z (Malvern Instruments, Malvern, UK). In addition, the average sizes of AuNS were determined via dynamic light scattering measurements using a Zetasizer Nano series instrument (Malvern Instruments, Malvern, UK). The absorbance spectra of each nanoparticle were obtained through UV-Vis spectrophotometry (UV 2550, Shimadzu, Japan). Each particle was irradiated using an 808 nm laser (diode laser, JENOPTIK unique-mode GmbH, Germany) with 2 W/cm^2 , and the temperature of each solution was measured with a thermocouple linked to a digital thermometer (Lutron Thermometer TM-917, Taiwan) for 5 min at 30 s intervals.

Cytotoxicity test of Dual-AuNS

Four cell lines (LNCaP, PC3, PNT2, and HeLa) were used to determine the cytotoxicity of the newly synthesized probe. Each cell line was cultured in RPMI-1640 supplemented with 10% (v/v) FBS, 100 U/mL penicillin G, and 100 mg/mL streptomycin at $37 \text{ }^\circ\text{C}$ in a 5% (v/v) CO_2 humid incubator. After the cells were cultured on a circular dish, the cells were

trypsinized and resuspended in serum-free RPMI-1640 media. Three microliters of 3×10^3 cells were sub-cultured to 80% (v/v) occupation on a 96-well plate in the humid CO₂ incubator. Each well was treated with various concentrations of Dual-AuNS (0.1, 0.2, and 0.3 nM) at 37 °C in the 5% (v/v) CO₂ humid incubator. The cell media was then replaced with 100 μL of fresh media and 10 μL of MTT solution (5 mg/mL), and the cells were incubated for 4 h at 37 °C. After the media was removed, 100 μL of DMSO was added to each well to liquefy the purple formazan crystals. The cell viability was measured three times at 570 nm using a microplate spectrofluorometer (VICTOR3 V Multilabel Counter). The MTT assay was carried out every 4 h (Fig. S1-S4).

Verification of the cellular uptake of Dual-AuNS

To access the selective cellular uptake of Dual-AuNS, three types of cell lines (LNCaP, PC3, and HeLa) were used. Each cell line was cultured on a 100 π dish according to the previously described conditions. When the cell confluency reached approximately 80% (v/v), 0.3 nM Dual-AuNS was applied to each plate. After washing with PBS buffer three times, each cell was transferred to a 1.5 mL tube in primary fixation buffer containing 2% paraformaldehyde, 2% glutaraldehyde, and 0.05 M sodium cacodylate (pH 7.2) at 4 °C and incubated for 4 h. Next, the cells were washed with 0.05 M sodium cacodylate buffer (pH 7.2) three times, incubated with the post-fixation buffer (1% osmium tetroxide and 0.05 M sodium cacodylate, pH 7.2) at 4 °C for 2 h, and subjected to *En bloc* staining with 0.5% uranyl acetate at 4 °C overnight. In addition, dehydration with EtOH and transition with propylene oxide were also performed. Additionally, the cells were infiltrated using a mixture of propylene oxide and Spurr's resin, polymerized, sectioned with an ultramicrotome (MT-X, RMC, Tucson, AZ, USA), and stained with 2% uranyl acetate and Reynold's lead citrate. TEM images of the cells treated with Dual-AuNS were taken using a JEM-1011 instrument (JEOL, Tokyo, Japan). Incubation time was also optimized via MTT assay (Fig. S5). Three types of cell lines (LNCaP, PC3, and HeLa) were incubated with 0.3 nM AuNS for various time and were irradiated using an 808 nm laser for 3 min (2 W/cm²).

Photothermal therapy

The selectivity of Dual-AuNS was demonstrated via photothermal therapy using six cell lines (positive targets: PC3 and LNCaP; negative control: PNT2, HeLa, MCF7, and A549). According to the previously described method, each cell line was grown to 80% (v/v) confluency on the 96-well plate. Then, 0.3 nM Dual-AuNS was added to the cells, and the cells were incubated at 37 °C for 24 h. The Dual-AuNS-treated cells were irradiated with an 808 nm laser under an irradiance of 2 W/cm². The cell viability was measured three times via the previously described MTT assay. Furthermore, the efficiency of Dual-AuNS was also proved. Dual-AuNS were incubated with the four cell lines (PC3, LNCaP, PNT2, and HeLa) at 37 °C for 24 h. Photothermal therapy was performed using various irradiation powers ranging from 4 to 0.3 W/cm². The MTT assay was also used to determine the cell viability. For the Trypan blue staining, the same experiment was conducted using only two cell lines (PC3 and LNCaP). The cells were incubated with Trypan blue solution (0.1%) for 5 min, washed with PBS, and subjected to microscopic analysis.

Results and discussion

Design of dual aptamer-modified gold nanostars

As illustrated in Fig. 1, Dual-AuNS were manufactured via several modification processes. AuNS were freshly synthesized using a seed-mediated method (Bare-AuNS) and were then swathed by mercaptopolyethylene glycol monomethyl ether (PEG-AuNS). Thiol-modified A10 (5'-thiol-GGGAGGACGAU GCGGAUCAGCCAUGUUUACGUCACUCCUUGUCAUUCUCAUCGGC-3') and cysteine-modified DUP-1 (CFRPNRAQ DYNTN) aptamers were introduced into PEG-AuNS via disulfide bonds at a ratio of 1:2, which can give rise to discrepancies in the photothermal ability for PSMA(+) and PSMA(-) cells, as was confirmed in our previous work.³²

Prior to photothermal therapy, Dual-AuNS were typified through a few analyses. The transmission electron microscopy (TEM) images clearly show the homogeneous distribution of Bare-AuNS and Dual-AuNS (Fig. 2a and 2b). The shape and size of the branches are relatively even, and the total form of AuNS is consistent. The immobilization of the aptamers on PEG-AuNS resulted in the particles being dispersed due to coulombic repulsion or steric hindrances between the aptamers. The average sizes of Bare-AuNS, PEG-AuNS, and Dual-AuNS determined by dynamic light scattering (DLS) were 39.19 ± 1.08 nm, 48.96 ± 0.98 nm, and 61.90 ± 1.61 nm, respectively. This sequential increase in size indicates the successful functionalization of AuNS. In addition, the ζ-potentials of AuNS were measured to quantify their surface charges. The ζ-potentials were -27.1 ± 1.3 mV (Bare-AuNS), -23.7 ± 0.8 mV (PEG-AuNS), and 9.6 ± 0.7 mV (Dual-AuNS). Because DUP-1 possesses relatively positive charge compared with A10 and AuNS, Dual-AuNS present more positive potential than the other particles. As represented in Fig. 2c, every type of AuNS exhibits high absorbance at a broad range of wavelengths (800 ~ 1000 nm), suggesting that it is appropriate to utilize an 808 nm laser for effective photothermal therapy. The heat generation capacity of 0.5 nM AuNS in PBS buffer was then demonstrated using 808 nm laser with an irradiation of 2 W/cm² (Fig. 2d). Although the heat generation of Dual-AuNS and PEG-AuNS was slightly lower than that of Bare-AuNS, an elevated temperature (>42 °C) was sufficient to kill malignant cells through apoptosis or necrosis.⁴³ All of these results indicate that well-synthesized Dual-AuNS are adequately applicable for hyperthermia therapy.

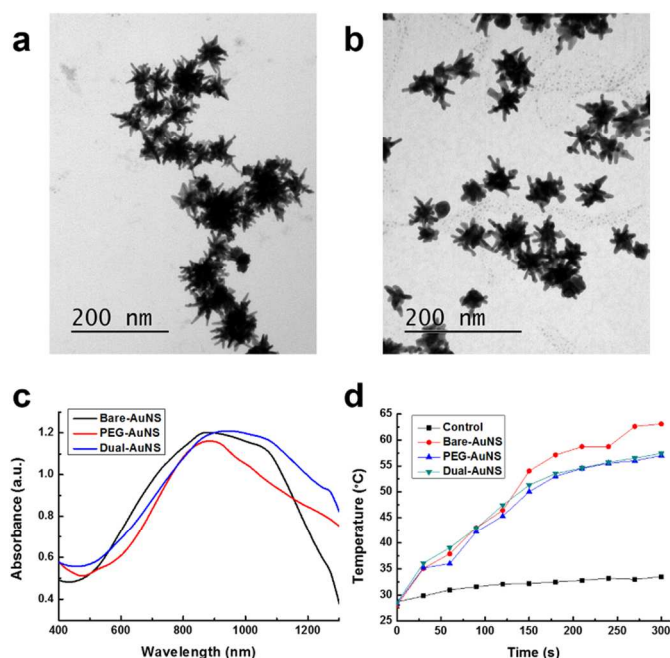


Fig. 2 Characterization of each AuNS. (a) TEM image of Bare-AuNS. (b) TEM image of Dual-AuNS. (c) Absorbance spectra of each type of AuNS. (d) Change in the temperature of PBS solutions containing 0.5 nM AuNS in response to NIR irradiation (808 nm, 2 W/cm²).

Cytotoxicity test of AuNS

Photothermal agents must not exhibit cytotoxicity for cancer cells in the absence of NIR irradiation. Therefore, before photothermolysis, the cytotoxicity of Dual-AuNS was evaluated by averaging the results of triplicate MTT assays (Fig. S1–S4). The following four cell lines were prepared on a 96-well plate until the cells reached 80% (v/v) confluency: PC3 as PSMA (–) prostate cancer cells, LNCaP as PSMA (+) prostate cancer cells, PNT2 as non-cancerous prostate cells, and HeLa as cervical cancer cells. The cell viability displayed no dependence on the concentration of Dual-AuNS and time, revealing that fabricated Dual-AuNS have no cytotoxicity. Though an increase in the concentration and longer incubation time can improve the therapeutic effect, concentration higher than 0.3 nM and prolonged incubation time influenced the cell viability. Hence, we employed Dual-AuNS at a concentration of 0.3 nM and incubation time of 24 h for therapy.

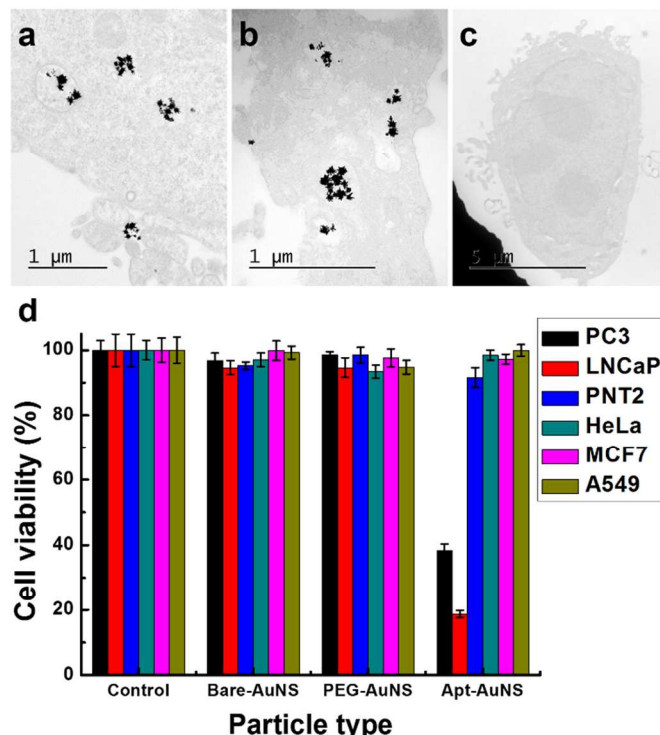


Fig. 3 (a) TEM image of PC3, (b) LNCaP, and (c) HeLa cells incubated for 24 h with 0.3 nM Dual-AuNS. (d) Selectivity test of Dual-AuNS. Six types of cell lines were incubated with 0.3 nM AuNS for 24 h and were irradiated using an 808 nm laser for 3 min (2 W/cm²). The cell viability was calculated through an MTT assay.

Confirmation of the selectivity of probes

To assess the selectivity of Dual-AuNS, three types of cancer cells, including PC3, LNCaP, and HeLa, were incubated with 0.3 nM Dual-AuNS for 24 h. The cells were washed with PBS three times, fixed, subjected to uranyl staining, and polymerized for TEM imaging. As shown in Fig. 3a–c, Dual-AuNS are only observed in the PSMA(+) and PSMA(–) cells, and almost all of the particles bunch up in small vesicles. It has been known that the A10 aptamer can be internalized to LNCaP by receptor-mediated endocytosis regardless of the presence of delivery vehicles and that the DUP-1 aptamer can also be localized in the cytoplasm via a fusion of the endocytotic vesicles to endosomes.^{29, 30} These features are precisely consistent with our results. Furthermore, Dual-AuNS were found only in the cytoplasmic part and not in intranuclear region, implying that comparatively large Dual-AuNS (~62 nm) are unable to pass through the nuclear pores (~50 nm) in accordance with previous results.^{44, 45} In addition to the TEM imaging analysis, incubation time was optimized via MTT assay. As shown in Fig. S5, although longer incubation time had the intracellular uptake efficiency higher, incubation time over 12 h was enough to carry out photothermal therapy. Therefore, we decided incubation time to be 24 h. Additionally, photothermolysis was carried out using six types of cell lines to prove the selectivity of the probe. PC3 and LNCaP cells were selected as positive targets, whereas PNT2 (normal prostate), HeLa, MCF7 (breast cancer), and A549 (lung cancer) cells were utilized as negative controls. After the cells were treated with each type of AuNS (0.3 nM) for 24 h, the remaining probes were eliminated through multiple washing, and the cells

were then exposed to NIR for 3 min. As shown in Fig. 3d, all of the cells exhibited the high cell viability in the presence of Bare-AuNS and PEG-AuNS, revealing that almost none of the nanoparticles were delivered sufficiently. This tendency coincides with the results of the previous study, which showed that native and PEGylated AuNS exhibit negligible cellular uptake due to aggregation or their large size.⁴⁶ In contrast, only PC3 and LNCaP cells incubated with Dual-AuNS exhibited a marked decrease in the cell viability. The difference in the viability between PC3 and LNCaP cells may originate from the inconsistency in the internalization capacity. Additionally, the weak expression of PSMA in PNT2 cells permits feeble binding of Dual-AuNS, resulting in a slight decrease in the viability of the cells incubated with the probes. These results clearly show that Dual-AuNS can simultaneously target PSMA(+) and PSMA(-) cells with great selectivity.

Verification of the efficiency of the particles

The efficiency of Dual-AuNS for photothermal therapy was verified employing four cell lines (PC3, LNCaP, prostate cancer; PNT2, normal prostate; HeLa, cervical cancer). When the cell confluency reached approximately 80% (v/v), the cells were incubated with Dual-AuNS for 24 h. Photothermal therapy was performed according to previously described conditions, with the exception of a different irradiation power. The cell viability as a function of the laser intensity was measured via an MTT assay. Fig. 4a undoubtedly indicates that an increase in the irradiation power improves the beneficial effect of the therapy. In particular, dual-aptamer conjugated AuNS represented quite effective capacity for photothermal therapy under an irradiation power of 0.3 W/cm², lower than the MPE of skin (0.329 W/cm²).³³ This high efficiency arises from the extreme intracellular uptake of aptamers. Although the cell viability of the control cells, such as PNT2 and HeLa, decreased slightly, this decrease was insignificant for the selectivity of Dual-AuNS. Moreover, the effect of hyperthermia therapy was demonstrated through Trypan blue staining. At 1 W/cm², large empty regions and dead cells stained by Trypan blue were detected in the irradiated region (Fig. 4b and 4c). Many free-floating cells detached from the plate were observed under the microscope. In the case of low irradiation, most of the cells were damaged and separated from the dish due to elevated temperature. Our result is the first substantiation of nanoparticle-based photothermal therapy with both extraordinary efficiency and extremely high selectivity for two types of prostate cancers synchronously.

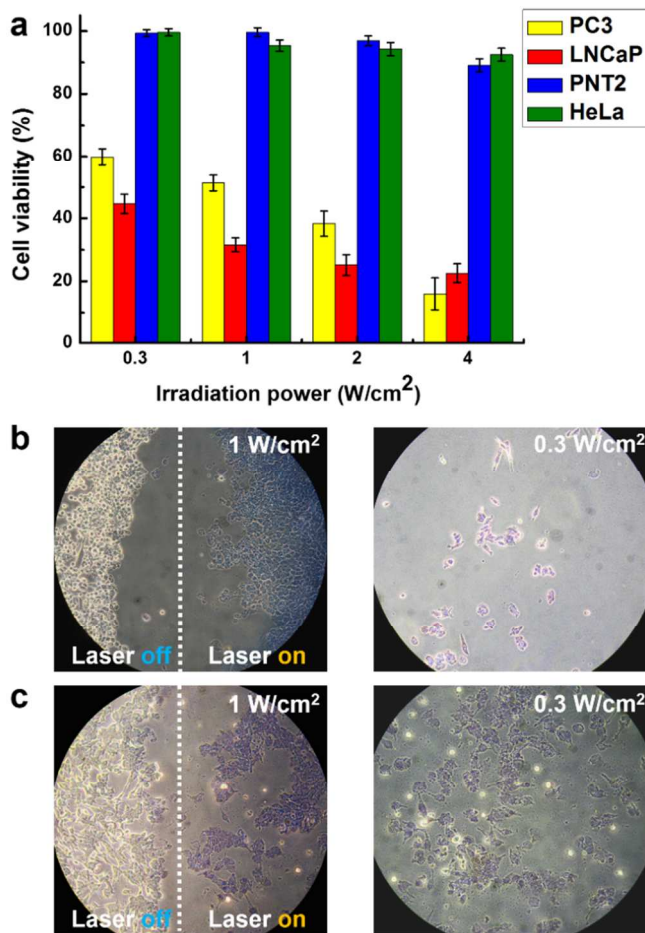


Fig. 4 (a) *In vitro* photothermal therapy using various irradiation powers. Four types of cell lines were incubated with 0.3 nM Dual-AuNS for 24 h, and were then irradiated with an 808 nm laser for 3 min. The cell viability was evaluated through an MTT assay. Trypan blue staining image of (b) PC3 and (c) LNCaP cells. The transparent and blue cells represent live and dead cells, respectively. The figures on the right are enlarged images of the irradiated region.

Conclusions

In summary, we have developed the first ultra-effective photothermal agents for prostate cancer-targeted therapy. The newly synthesized probe was found to be intensely and specifically accumulated into PSMA(+) and PSMA(-) cells without any impact on the cell viability, resulting in tremendously efficient targeted therapy. To apply this probe *in vivo* therapies, we have made an effort to overcome various problems, such as short half-life of the particles in the circulation, low permeability of them, and instability of aptamers in the blood. It is expected that successful further study makes aptamer-modified AuNS the promising *in vivo* therapeutic nanomaterials for the treatment of not only prostate cancers but also other carcinomas.

Acknowledgements

We thank Prof. W.J. Kim and H. Kim for their kind offer of the NIR equipment and the zeta potential instrument. This work was supported by the National Research Foundation of Korea (NRF-2013008202) and a grant of the Korean Health

Technology R&D Project, Ministry of Health & Welfare, Republic of Korea (A122001-1211-0000200).

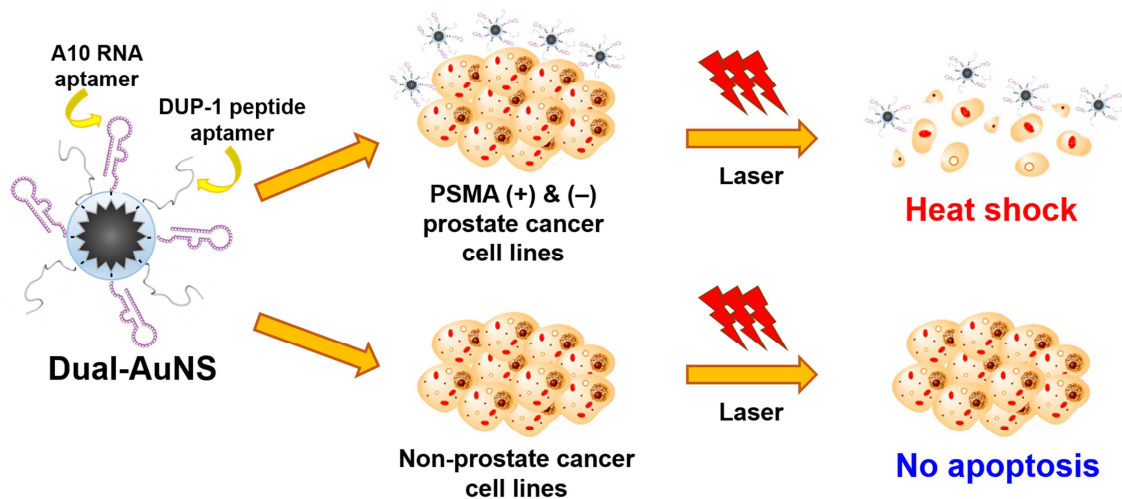
Notes and references

Department of Chemistry, Pohang University of Science and Technology, 77, Cheongam-Ro, Nam-Gu, Pohang, Gyeongbuk, 790-784, Korea.

† Electronic Supplementary Information (ESI) available: cytotoxicity test of Dual-AuNS. See DOI: 10.1039/b000000x/

§ These authors contributed equally to this work.

- M. Markman, B. Reichman, T. Hakes, J. Curtin, W. Jones, J. L. Lewis, Jr., R. Barakat, S. Rubin, B. Mychalczak, P. Saigo and et al., *Cancer*, 1993, **71**, 1565-1570.
- K. K. Fu, T. F. Pajak, A. Trotti, C. U. Jones, S. A. Spencer, T. L. Phillips, A. S. Garden, J. A. Ridge, J. S. Cooper and K. K. Ang, *Int. J. Radiat. Oncol. Biol. Phys.*, 2000, **48**, 7-16.
- P. J. Hesketh, *N. Engl. J. Med.*, 2008, **358**, 2482-2494.
- J. Crawford, H. Ozer, R. Stoller, D. Johnson, G. Lyman, I. Tabbara, M. Kris, J. Grous, V. Picozzi, G. Rausch and et al., *N. Engl. J. Med.*, 1991, **325**, 164-170.
- C. Dees, J. Harkins, M. G. Petersen, W. G. Fisher and E. A. Wachter, *Photochem. Photobiol.*, 2002, **75**, 296-301.
- B. Samanta, H. Yan, N. O. Fischer, J. Shi, D. J. Jerry and V. M. Rotello, *J. Mater. Chem.*, 2008, **18**, 1204-1208.
- Y. Xu, W. E. Heberlein, M. Mahmood, A. I. Orza, A. Karmakar, T. Mustafa, A. R. Biris, D. Casciano and A. S. Biris, *J. Mater. Chem.*, 2012, **22**, 20128-20142.
- S. D. Brown, P. Nativo, J. A. Smith, D. Stirling, P. R. Edwards, B. Venugopal, D. J. Flint, J. A. Plumb, D. Graham and N. J. Wheate, *J. Am. Chem. Soc.*, 2010, **132**, 4678-4684.
- S. Jelveh and D. B. Chithrani, *Cancers*, 2011, **3**, 1081-1110.
- D. B. Chithrani, S. Jelveh, F. Jalali, M. van Prooijen, C. Allen, R. G. Bristow, R. P. Hill and D. A. Jaffray, *Radiat. Res.*, 2010, **173**, 719-728.
- L. Rodriguez-Lorenzo, R. A. Alvarez-Puebla, F. J. G. de Abajo and L. M. Liz-Marzan, *J. Phys. Chem. C*, 2010, **114**, 7336-7340.
- W. Ahmed, E. S. Kooij, A. van Silfhout and B. Poelsema, *Nanotechnology*, 2010, **21**, 125605.
- H. K. Yuan, C. G. Khoury, H. Hwang, C. M. Wilson, G. A. Grant and T. Vo-Dinh, *Nanotechnology*, 2012, **23**, 075102.
- E. Hao, R. C. Bailey, G. C. Schatz, J. T. Hupp and S. Y. Li, *Nano Lett.*, 2004, **4**, 327-330.
- B. Van de Broek, N. Devoogdt, A. D'Hollander, H. L. Gijs, K. Jans, L. Lagae, S. Muyltermans, G. Maes and G. Borghs, *Acs Nano*, 2011, **5**, 4319-4328.
- D. H. M. Dam, J. H. Lee, P. N. Sisco, D. T. Co, M. Zhang, M. R. Wasielewski and T. W. Odom, *Acs Nano*, 2012, **6**, 3318-3326.
- H. K. Yuan, C. G. Khoury, C. M. Wilson, G. A. Grant, A. J. Bennett and T. Vo-Dinh, *Nanomed.-Nanotechnol.*, 2012, **8**, 1355-1363.
- R. Siegel, E. Ward, O. Brawley and A. Jemal, *Ca-Cancer J. Clin.*, 2011, **61**, 212-236.
- P. D. Baade, D. R. Youlten and L. J. Krnjacki, *Mol. Nutr. Food Res.*, 2009, **53**, 171-184.
- G. P. Murphy, T. G. Greene, W. T. Tino, A. L. Boynton and E. H. Holmes, *J. Urol.*, 1998, **160**, 2396-2401.
- S. S. Chang, V. E. Reuter, W. D. Heston and P. B. Gaudin, *Urology*, 2001, **57**, 1179-1183.
- S. D. Sweat, A. Pacelli, G. P. Murphy and D. G. Bostwick, *Urology*, 1998, **52**, 637-640.
- A. Ghosh and W. D. Heston, *J. Cell. Biochem.*, 2004, **91**, 528-539.
- R. S. Israeli, C. T. Powell, J. G. Corr, W. R. Fair and W. D. Heston, *Cancer Res.*, 1994, **54**, 1807-1811.
- P. F. Kue, J. S. Taub, L. B. Harrington, R. D. Polakiewicz, A. Ullrich and Y. Daaka, *Int. J. Cancer*, 2002, **102**, 572-579.
- J. M. Carothers, S. C. Oestreich and J. W. Szostak, *J. Am. Chem. Soc.*, 2006, **128**, 7929-7937.
- S. M. Nimjee, C. P. Rusconi and B. A. Sullenger, *Annu. Rev. Med.*, 2005, **56**, 555-583.
- D. Proske, M. Blank, R. Buhmann and A. Resch, *Appl. Microbiol. Biotechnol.*, 2005, **69**, 367-374.
- S. E. Lupold, B. J. Hicke, Y. Lin and D. S. Coffey, *Cancer Res.*, 2002, **62**, 4029-4033.
- S. Zitzmann, W. Mier, A. Schad, R. Kinscherf, V. Askoxyllakis, S. Kramer, A. Altmann, M. Eisenhut and U. Haberkorn, *Clin. Cancer Res.*, 2005, **11**, 139-146.
- K. Min, H. Jo, K. Song, M. Cho, Y. S. Chun, S. Jon, W. J. Kim and C. Ban, *Biomaterials*, 2011, **32**, 2124-2132.
- K. Min, K. M. Song, M. Cho, Y. S. Chun, Y. B. Shim, J. K. Ku and C. Ban, *Chem. Commun.*, 2010, **46**, 5566-5568.
- ANSI, *American National Standard for safe use of lasers*, Laser Institute of America: Orlando, FL, 2000.
- J. Kim, S. Park, J. E. Lee, S. M. Jin, J. H. Lee, I. S. Lee, I. Yang, J. S. Kim, S. K. Kim, M. H. Cho and T. Hyeon, *Angew. Chem.*, 2006, **45**, 7754-7758.
- L. Au, D. Zheng, F. Zhou, Z. Y. Li, X. Li and Y. Xia, *Acs Nano*, 2008, **2**, 1645-1652.
- E. B. Dickerson, E. C. Dreaden, X. Huang, I. H. El-Sayed, H. Chu, S. Pushpanketh, J. F. McDonald and M. A. El-Sayed, *Cancer Lett.*, 2008, **269**, 57-66.
- J. Y. Chen, C. Glaus, R. Laforest, Q. Zhang, M. X. Yang, M. Gidding, M. J. Welch and Y. N. Xia, *Small*, 2010, **6**, 811-817.
- A. M. Gobin, E. M. Watkins, E. Quevedo, V. L. Colvin and J. L. West, *Small*, 2010, **6**, 745-752.
- W. Lu, C. Xiong, G. Zhang, Q. Huang, R. Zhang, J. Z. Zhang and C. Li, *Clin. Cancer Res.*, 2009, **15**, 876-886.
- H. Yuan, A. M. Fales and T. Vo-Dinh, *J. Am. Chem. Soc.*, 2012, **134**, 11358-11361.
- J. J. Storhoff, R. Elghanian, R. C. Mucic, C. A. Mirkin and R. L. Letsinger, *J. Am. Chem. Soc.*, 1998, **120**, 1959-1964.
- P. C. Patel, D. A. Giljohann, D. S. Seferos and C. A. Mirkin, *Proc. Natl. Acad. Sci. U. S. A.*, 2008, **105**, 17222-17226.
- M. W. Dewhirst, Z. Vujaskovic, E. Jones and D. Thrall, *Int. J. Hyperthermia*, 2005, **21**, 779-790.
- L. Pan, Q. He, J. Liu, Y. Chen, M. Ma, L. Zhang and J. Shi, *J. Am. Chem. Soc.*, 2012, **134**, 5722-5725.
- C. C. Berry, J. M. de la Fuente, M. Mullin, S. W. Chu and A. S. Curtis, *IEEE Trans. Nanobioscience*, 2007, **6**, 262-269.
- R. Levy, U. Shaheen, Y. Cesbron and V. See, *Nano Rev.*, 2010, **1**.



A novel general platform for disease-specific photothermal therapy. This is the first demonstration of gold nanostars with tremendous efficiency and impressive selectivity for the targeted cancer, particularly the simultaneous targeting of PSMA(+) and PSMA(-) prostate cancers. The PEGylation and dual-aptamer modification make the nanoparticles stable and permeable to cancers, resulting in the prominent outcome.